MASTER

PREPRINT UCRL-80469

CONF-780503--2

Lawrence Livermore Laboratory

MATERIALS TESTING USING LASER ENERGY DEPOSITION

W.W. Wilcox

C. A. Calder

December 20, 1977

This paper was prepared for submission to
24th International Instrumentation Symposium
Albuquerque, NM, May 1-4, 1978

MATERIALS TESTING USING LASER ENERGY DEPOSITION

W. W. Wilcox
Technical Associate
Lawrence Livermore Laboratory
Livermore, California

Clarence Calder
Engineer
Lawrence Livermore Laboratory
Livermore, California

ABSTRACT

A convenient method for determining the elastic constants of materials has been devised using the energy from a Q-switched neodymium-glass laser. Stress waves are induced in materials having circular rod or rectangular bar geometries by the absorption of energy from the laser. The wave transit times through the material are recorded with a piezoelectric transducer. Both dilatation and shear wave velocities are determined in a single test using an ultrasonic technique and these velocities are used to calculate the elastic constants of the material. A comparison of the constants determined for ten common engineering materials using this method is made with constants derived using the conventional ultrasonic pulse technique and agreement is shown to be about one percent in most cases. Effects of material geometry are discussed and surface damage to the material caused by laser energy absorption is shown.

INTRODUCTION

The pulsed laser has been used by a number of investigators to explore a variety of experimental situations in which stress waves are generated in a material by rapid absorption of energy[1-6]. It is known that surface vaporization and heating can occur in various materials on time scales comparable to the laser pulse width. This rapid deposition of energy into the material results in an unbalanced stress state which produces a stress gradient that will propagate through the material. This "laser induced stress pulse" will travel through the material at a velocity which is dependent upon the density of the material, its elastic constants, and the direction of propagation. By varying the energy and pulse width of the laser and by using various methods to couple the energy to the material the type of stress wave generated will vary from elastic to plastic to hydrodynamic. When an elastic wave is generated along the axis of a circular rod where the diameter is large in comparison to the wavelength of the pulse, it will travel down the rod at the material's characteristic dilatational velocity. As the dilatational wave grazes the lateral boundary of the rod part of its energy is continually "mode converted" to a shear wave, which travels across the rod and is converted to a shear and dilatational wave upon striking the opposite boundary. This mode conversion described by Hughes[7] et al and later applied by Reynolds[8] and Dunegan[9] permits the evaluation of the shear velocity of the specimen, and leads ultimately to the evaluation of the elastic constants of the material. Laser generated stress waves traveling at dilatational velocity were first experimentally verified by Percival[10-11] in the late 1960's and he later applied this in the determination of the elastic constants of 2024 aluminum at elevated temperature using the "mode conversion" concept described by Hughes. In the present study a variety of materials having circular rod or rectangular bar geometries are subjected to laser energy deposition and the measurement of the generated stress wave velocities are used to determine the elastic constants of these materials.

WAVE VELOCITY AND ELASTIC CONSTANTS EQUATIONS

The classical theory of isotropic elasticity shows that

$$V_S = \left(\frac{\mu}{\rho}\right)^{1/2} \tag{1}$$

and

$$V_D = \left(\frac{\lambda+2\mu}{\rho}\right)^{1/2} = \left(\frac{K+2\mu/3}{\rho}\right)^{1/2} =$$

$$\left[\left(\frac{\mu}{\rho}\right)\left(\frac{4\mu-E}{3\mu-E}\right)\right]^{1/2} = \left[\left(\frac{E}{\rho}\right)\left(\frac{1-\nu}{(1+\nu)(1-2\nu)}\right)\right]^{1/2} \tag{2}$$

where

V_S = shear velocity

V_D = dilatational velocity

ρ = mass density of the sample

μ = shear modulus

E = Young's modulus

k = bulk modulus

ν = Poisson's ratio

λ = Lame's constant

As only two of the elastic constants are independent, the evaluation of V_D and V_S will lead to any of the five elastic constants desired.

Letting T be the transit time of the dilatational pulse through the sample and Δt the mode converted pulse separation from the dilatational pulse it can be shown that:

$$\Delta t = \frac{D}{V_S V_D}\left(V_D^2 - V_S^2\right)^{1/2} \tag{3}$$

$$\text{and } V_D = \frac{L}{T} \tag{4}$$

where D = sample diameter or lateral dimension

and L = sample length

The shear velocity can then be found from the expression

$$V_S = \frac{DV_D}{(D^2+V_D^2\Delta t^2)^{1/2}} \tag{5}$$

By defining the velocity ratio as

$$r = \frac{V_D}{V_S} \tag{6}$$

the five elastic constants are found in the following manner.

$$\mu = \rho V_S^2 \tag{7}$$

$$\nu = \frac{1-\frac{r^2}{2}}{1-r^2} \tag{8}$$

$$E = \rho V_S^2\left(\frac{4-3r^2}{1-r^2}\right) \tag{9}$$

$$k = \rho V_S^2\left(r^2-4/3\right) \tag{10}$$

$$\lambda = \rho V_S^2\left(r^2-2\right) \tag{11}$$

SYSTEM DESIGN AND PROCEDURE

The experimental arrangement used in determining the elastic constants of the various specimens is shown schematically in Figure 1. The He-Ne alignment laser was used to position the specimen in the beam path of the pulsed Nd-glass laser. The Nd-glass laser is capable of a maximum of 15 Joules with a 30 ns pulse width. Typical levels used in the experiment varied from 7-10 Joules. This resulted in a power density at the specimen of about 0.2 GW/cm^2. A thin glass beam splitter was placed in the Nd-glass laser path at 45° to direct a portion of the laser pulse to a photo-diode. The photo-diode provided a zero-time trigger to the high speed oscilloscope. The oscilloscope received signals from a 10 MHz ultrasonic transducer which was wrung on the back of the specimens to sense the stress wave arrival times. The stress wave arrival times were recorded using an oscilloscope operated in a single sweep mode and a polaroid camera. Extremely accurate delay times were set on the oscilloscope using a digital delay plug-in unit. The time base and digital delay unit were both calibrated and the accuracy of the sweep was maintained to approximately 2% full scale. Specimen preparation consisted of machining both ends flat. Length, diameter and lateral dimensions were accurately measured and recorded. The densities of the samples were determined using the water immersion technique. When the 2.54 cm diameter circular rod samples were prepared, a .62 cm thick section was machined from each specimen for use in the conventional ultrasonic pulse method of determining the elastic constants. Aluminum samples of four different sizes were prepared in order to investigate the effects of geometry on the stress wave pulse shape. Rectangular bar samples of aluminum were also prepared with four different geometries in order to show the effect that varying the ratio of the lateral dimensions had on the mode converted stress pulse arrival times. The measured arrival times of the stress pulses were then used with equations 4 and 5 to determine the dilatational and shear velocities. The velocity ratio was then determined using equation 6 and the elastic constants derived using equations 7-11. To facilitate computations, a program was written for a programmable hand calculator.

EXPERIMENTAL RESULTS AND DISCUSSION

The elastic constants for ten materials determined using both the conventional ultrasonic pulse technique and the laser generated stress wave method are shown in Table 1. Agreement between the two methods is generally within 1-2% although some higher deviations occur as the result of the frequency dependence of the sound velocities as measured when using the ultrasonic pulse method. Figure 2 shows the arrival times and pulse shapes for the four different geometries of aluminum rods. The stress wave arrival times were as predicted for all geometries, however the makeup of the signal varied significantly as the rod diameter decreased. As the diameter decreased the number of cycles in the arriving signal increased and concurrently the amplitude of the mode converted pulse increased. The increase in the number of cycles appears to be due to the increased dispersion and mode conversions that occur in the smaller diameter rods. The increase in the amplitude of the mode converted pulse is due to the increased percentage of energy that this pulse is able to transmit across the smaller diameter. Figure 3 shows the stress wave arrival times for the aluminum rectangular bar geometries. These bars were used to demonstrate the ability to use specimens of geometries other than a circular rod. As long as an adequate length to lateral dimension ratio is maintained, the clear arrival times of the initial mode converted pulses will be unaffected by subsequent arrivals of reflected dilatational pulses. While the aluminum is an isotropic material, it appears that the rectangular bar geometry may be used with an anisotropic material to determine its elastic constants in a similar manner. Figure 4 shows the recorded stress pulse arrival times for three non-metallic samples. One of the advantages of the laser generated stress wave method of determining elastic constants is its ability to deliver enough energy to drive a stress pulse through a large sample of highly attenuating material. The non-metallic samples tend to show the greatest deviation in compared elastic constants. This is to be expected as a result of the inhomogeniety and frequency dependence of these samples as compared to metallic samples. We believe that the elastic constants determined for the non-metallic samples using the laser generated stress wave method tend to be more representative of the sample as a whole. Figure 5 shows the surface damage to aluminum and stainless steel caused by energy absorption from the laser. This qualitative study was done to provide cursory information regarding the use of the laser generated stress wave method to determine elastic constants of serviceable parts. The upper photographs show the entire area affected by the laser input. The remaining four photographs were taken using a scanning electron microscope. The photographs show that minimal surface damage occurs. While there is melting and probable material removal, the quantities involved are in the micro-inch and micro-gram scale and therefore would not affect the serviceability of a part.

CONCLUSIONS

The use of laser generated stress waves to evaluate wave velocites and corresponding elastic constants of materials of varying geometry and composition has been successfully demonstrated. Qualitative scanning electron microscope photographs indicate minimal surface damage. The experimental arrangement used permits rapid testing of a variety of samples. The values of the elastic constants correspond closely in most cases to those determined ultrasonically and with previously published values. Effects of geometry have been explored and the results of varying the diameter of the circular rod specimens indicate increased dispersion with diminishing diameters but no change in expected wave velocities. The rectangular bar specimens point out the ability to determine the mode converted wave velocities from each lateral direction and point out the possibility of using this technique to test anisotropic specimens with similar geometries. The high energy input of this method also makes it attractive for use with highly dispersive or attenuating media such as plastics, rocks, coal and oil shale and fiber composites.

ACKNOWLEDGEMENT

This work was performed under the auspices of the U.S. Department of Energy under contract No. W7405-Eng-48.

REFERENCES

(1) Anderholm, Curtis N., "Laser Generated Stress Waves", Applied Physics Letters, Vol. 16, No. 3, Feb. 1970, 113-115.

(2) Calder, C. A. and Wilcox, W. W., "Applications of Laser Induced Stress Waves", Lawrence Livermore Laboratory, Report UCID-16353, 1973.

(3) Calder, C. A. and Wilcox, W. W., "Technique for Measurement of Elastic Constants by Laser Energy Deposition", Review of Scientific Instruments, Vol. 45, No. 12, Dec. 1974, 1557-1559.

(4) Palmer, A. J. and Asmus J. F., "A Study of the Homogenization and Dispersion of Laser Induced Stress Waves", Applied Optics, Vol. 9, No. 1, Jan. 1970, 227-229.

(5) Skeen, C. H. and York, C. M., "Laser Induced Blowoff Phenomena", Applied Physics Letters, Vol. 12, No. 11, June 1968, 369-371.

(6) O'Keefe, J. D. and Skeen, C. H., "Laser Induced Stress Wave and Impulse Augmentation", Applied Physics Letters, Vol. 21, No. 10, Nov. 1972, 464-466.

(7) Hughes, D. S., Pondrom, W. L., and Mims, R. L., "Transmission of Elastic Pulses in Metal Rods", Physical Review, Vol. 75, 1949, 1552-1556.

(8) Reynolds, Myron B., "The Determination of the Elastic Constants of Metals by the Ultrasonic Pulse Technique", Transactions of the A.S.M., Vol. 45, 1953, 839.

(9) Dunegan, H. L., "High Temperature Dynamic Modulus Measurements by Use of Ultrasonics", Materials Evaluation, Vol. 22, 1960, 266-272.

(10) Percival, C. M., "Thermally Generated Stress Waves in a Dispersive Elastic Rod", Lawrence Livermore Laboratory, Report UCRL-50252, 1967.

(11) Brammer, J. A. a d Percival, C. M., "Elevated-temperature Elastic Moduli of 2024 Aluminum Obtained by a Laser-pulse Technique", Experimental Mechanics, Vol. 10, June 1970, 245-250.

Material	Method	V_D m/sec	V_S m/sec	Young's Modulus GPa	Poisson's Ratio	Shear Modulus GPa	Bulk Modulus GPa
1100 Al	Laser	6460	3051	68.56	.356	25.27	79.58
	Ultrasonic	6433	3086	69.78	.350	25.83	77.83
6061 Al	Laser	6398	3086	69.49	.343	25.77	76.37
	Ultrasonic	6444	3142	71.74	.344	26.69	76.68
304 S.S.	Laser	5819	3048	191.7	.311	73.12	169.1
	Ultrasonic	5805	3054	192.1	.308	73.39	167.4
Copper	Laser	4774	2280	125.7	.352	46.47	141.9
	Ultrasonic	4730	2276	124.9	.349	46.29	138.2
1018 Steel	Laser	5923	3225	210.8	.289	81.74	166.8
	Ultrasonic	5929	3234	211.6	.288	82.16	166.6
Brass	Laser	4369	2038	95.8	.361	35.22	114.8
	Ultrasonic	4337	2176	106.8	.332	40.29	105.9
Phenolic Canvas	Laser	3473	1424	7.59	.399	2.71	12.52
	Ultrasonic	3159	1374	6.99	383	2.52	9.98
Nylon	Laser	2665	1059	3.63	.406	1.29	6.45
	Ultrasonic	2659	1102	3.90	.396	1.40	6.28
Tantalum	Laser	4165	2002	184.1	.350	68.30	204.4
Tungsten	Laser	5210	2816	391.9	.294	151.5	316.4

TABLE 1 Elastic Constants

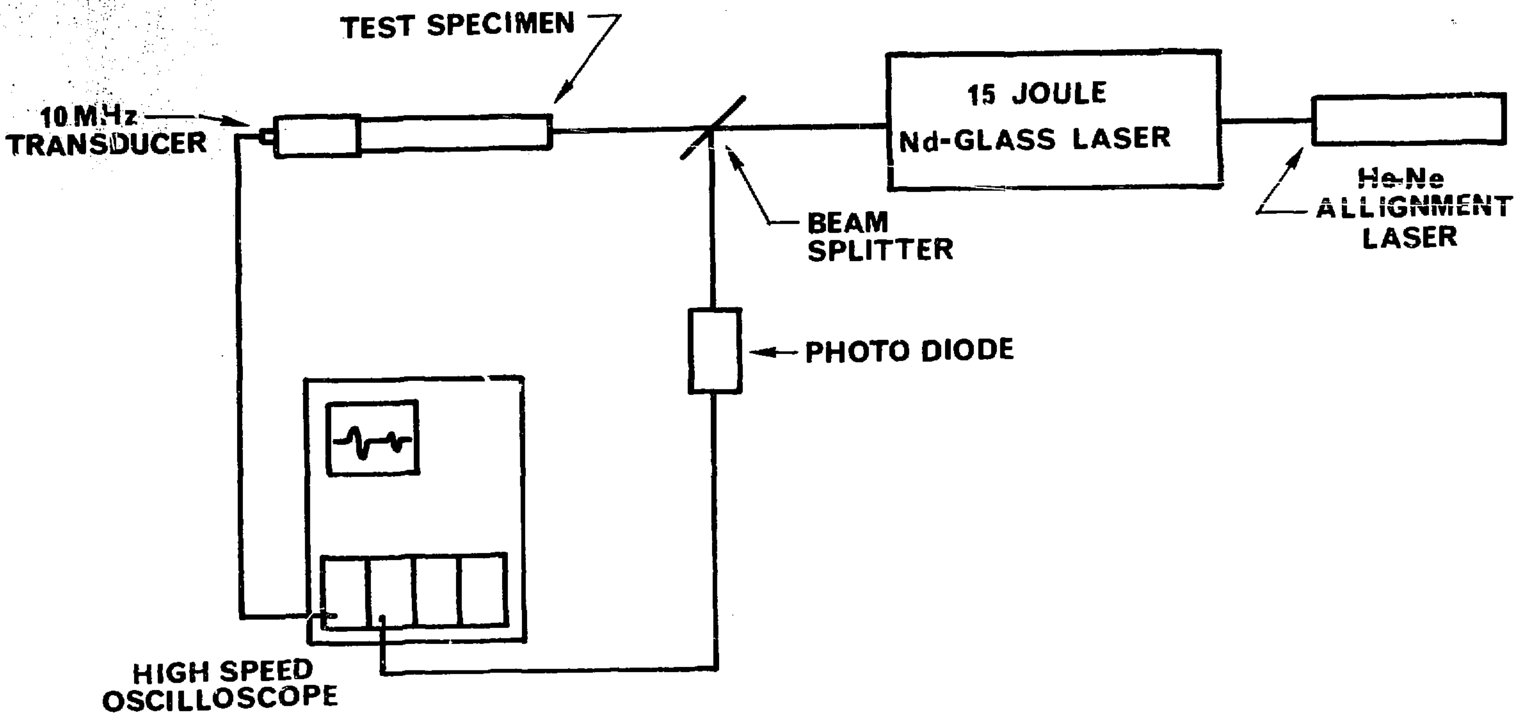

FIG.1 EXPERIMENTAL ARRANGEMENT

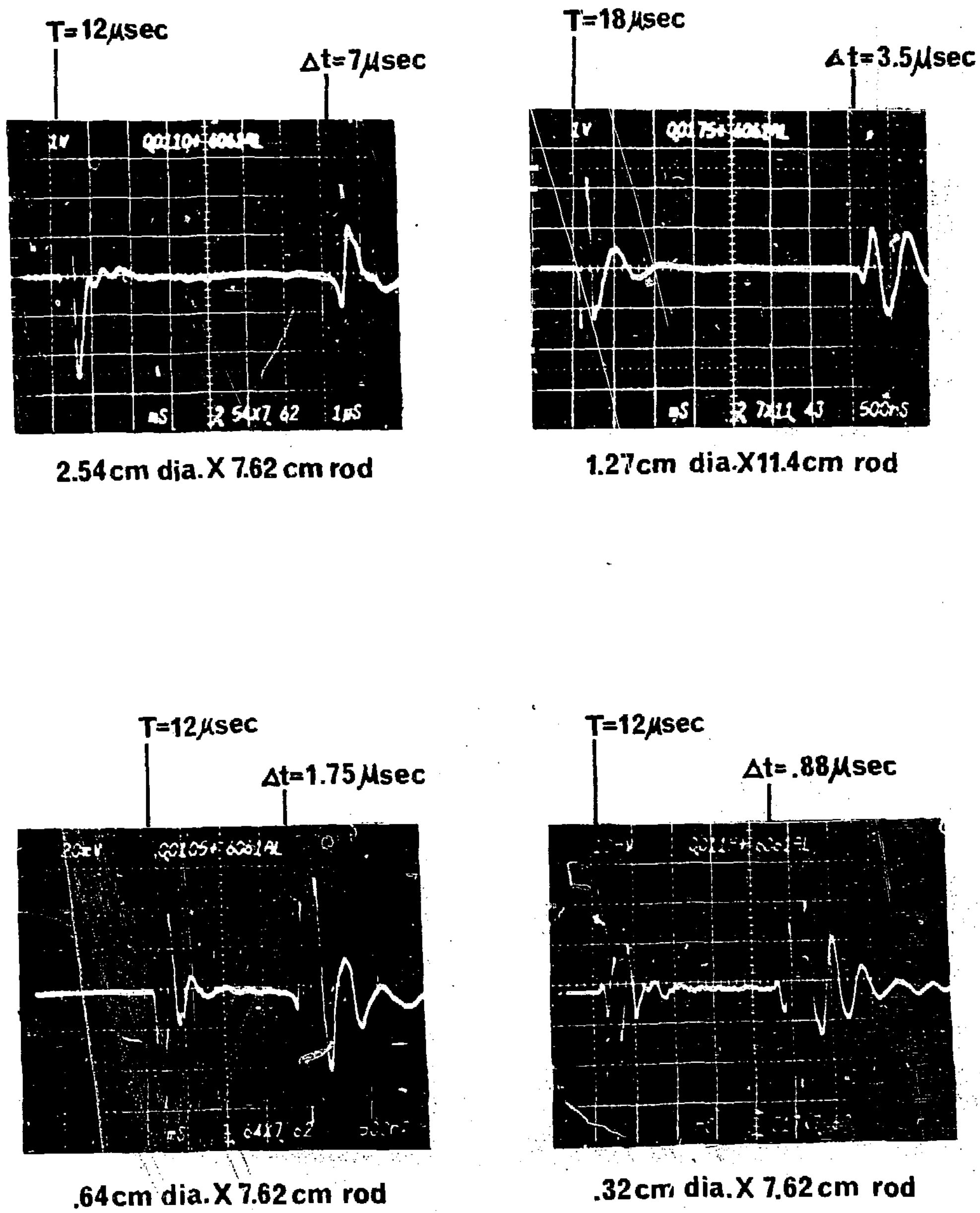

FIG. 2 Aluminum Circular Rod Geometries

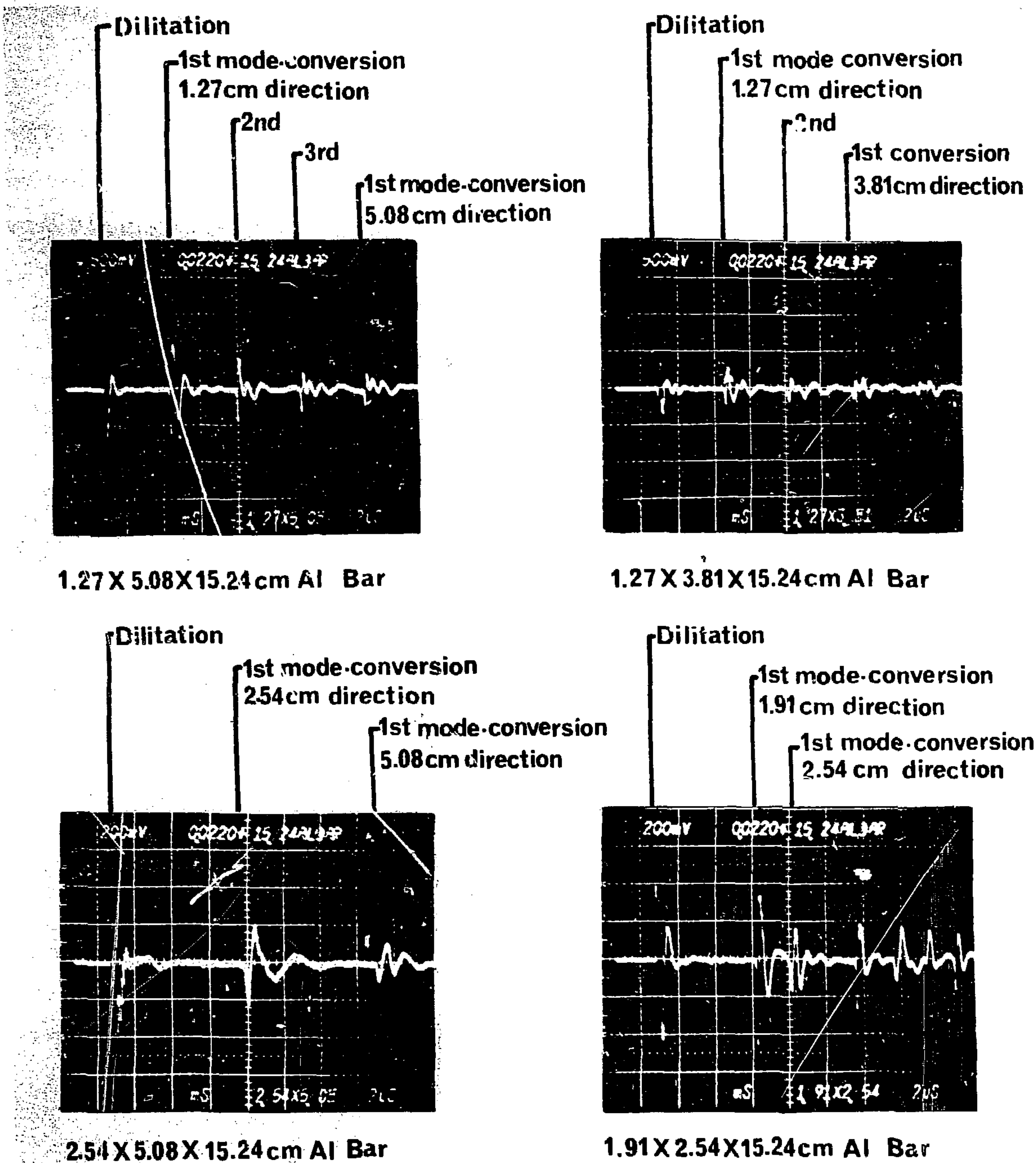

FIG.3 Rectangular Bar Geometries

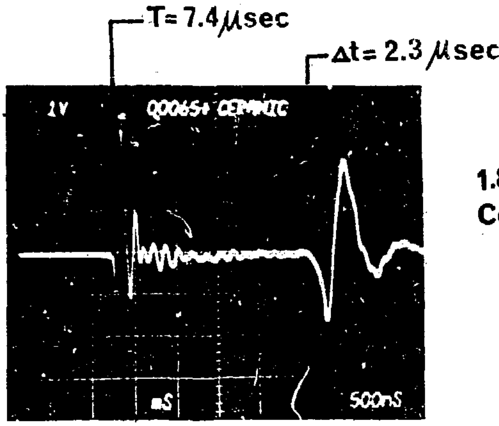

1.82cm dia.X 7.45cm long
Ceramic Rod

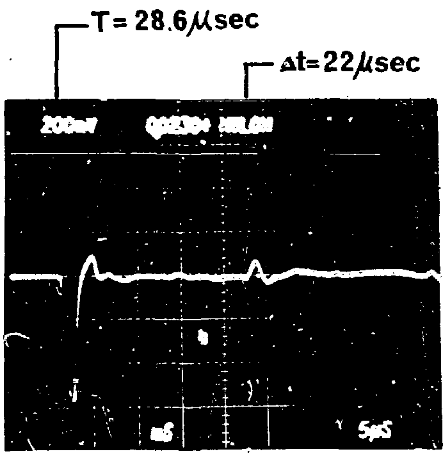

2.54cm dia.X 7.62cm long
Nylon Rod

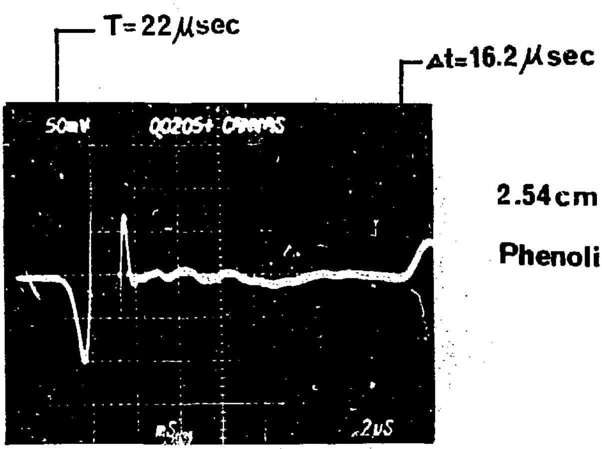

2.54cm dia.X 7.62 cm long
Phenolic Canvas Rod

FIG.4 NON-Metallic Specimens

2.54 cm dia. Al, Normal Photo

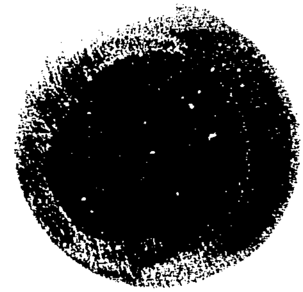

2.54 cm dia. 304 S.S. Normal Photo

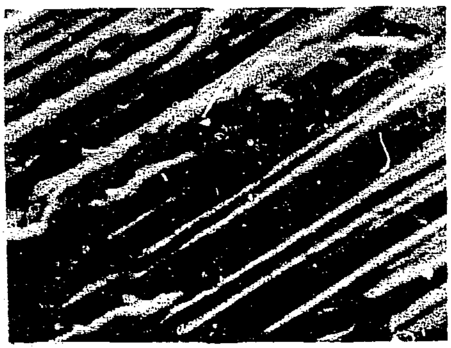

900X SEM Photo, unirradiated Al

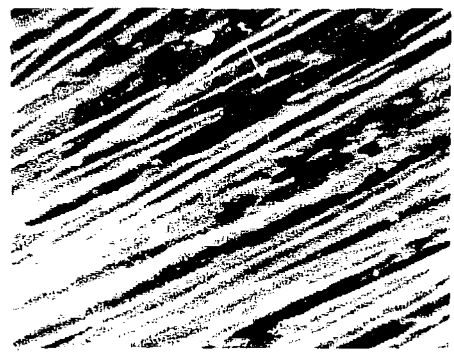

900X SEM Photo, unirradiated 304 S.S.

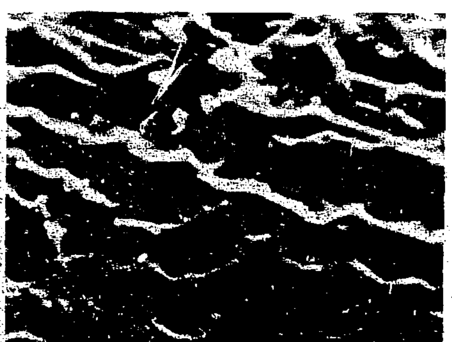

900X SEM Photo, irradiated Al

900X SEM Photo, irradiated 304 S.S.

FIG.5 Laser Induced Surface Damage